Analysis of the cure reaction of carbon nanotubes/epoxy resin composites through thermal analysis and Raman spectroscopy. J Appl Polym Sci

ARTICLE *in* JOURNAL OF APPLIED POLYMER SCIENCE · APRIL 2003

Impact Factor: 1.77 · DOI: 10.1002/app.11745

3 AUTHORS, INCLUDING:

Debora Puglia
Università degli Studi di Perugia
114 PUBLICATIONS **1,423** CITATIONS
SEE PROFILE

Jose M. Kenny
Università degli Studi di Perugia
631 PUBLICATIONS **10,194** CITATIONS
SEE PROFILE

Analysis of the Cure Reaction of Carbon Nanotubes/Epoxy Resin Composites Through Thermal Analysis and Raman Spectroscopy

D. Puglia, L. Valentini, J. M. Kenny

Materials Engineering Center, University of Perugia, 05100 Terni, Italy

Received 13 March 2002; accepted 4 June 2002

ABSTRACT: The effect of the incorporation of single-walled carbon nanotubes (SWNTs) onto a diglycidyl ether of bisphenol A-based (DGEBA) epoxy resin cure reaction was investigated by thermal analysis and Raman spectroscopy. The results of the investigation show that SWNTs act as a strong catalyst. A shift of the exothermic reaction peak to lower temperatures is, in fact, observed in the presence of SWNTs. Moreover, these effects are already noticeable at the lowest SWNT content investigated (5%) with slight further effects at higher concentrations, suggesting a saturation of the catalyzing action at the higher concentrations studied. The curves obtained under isothermal conditions confirm the results obtained in nonisothermal tests showing that the cure reaction takes less time with respect to the neat epoxy. The thermal degradation of cured DGEBA and DGEBA/SWNT composites was examined by thermogravimetry, showing a faster thermal degradation for DGEBA–SWNT composites. Raman spectroscopy was successfully applied to demonstrate that the observed changes in the cure reaction of the composites lead to a different residual strain on the SWNT bundles following a different intercalation of the epoxy matrix. © 2003 Wiley Periodicals, Inc. J Appl Polym Sci 88: 452–458, 2003

Key words: nanocomposites; differential scanning calorimetry (DSC); Raman spectroscopy

INTRODUCTION

The discovery of carbon nanotubes (CNTs) and carbon nanostructured materials has inspired scientists to consider them for a range of potential applications.[1–4] More specifically, the use of CNTs in polymer/CNT composites has attracted wide attention in terms of particular mechanical and electric properties.[5,6] CNTs, in fact, have a unique atomic structure, very high aspect ratio, and extraordinary mechanical properties (strength and flexibility), as directly measured using transmission electron microscopy,[7] making them ideal reinforcing fibers in nanocomposites. In this sense, it has been reported that the addition of CNTs in different polymer matrices do have some effective enhancement on the matrix properties.[5,8–10] On the other hand, epoxy resins are well established as thermosetting matrices of advanced composites, displaying a series of interesting characteristics, which can be adjusted within broad boundaries.[11–15] They are used as high-grade synthetic resins, for example, in the electronics, aeronautics, and astronautics industries. Through modification of the hardener systems and appropriate structural fibers for reinforcement, their properties can be adapted to the particular application. They are distinguished by good bond strength on the most varied materials, a comparatively low thermal expansion, good chemical resistance, and excellent electrical, mechanical, and thermal properties. The incorporation of CNTs as reinforcement will surely enhance the properties of epoxy resins but would also modify their processing behavior.

The study of cure kinetics is of great importance in polymer processing. In particular, the study of the cure reactions of polymers as a function of the processing conditions, from a macrokinetic point of view, is very important for the analysis and design of processing operations. On the other hand, physical properties of polymeric materials strongly depend on their microstructure, since it is at this microscopic level where failure of the materials takes place. Calorimetry may be considered as one of the most interesting techniques for macrokinetic analysis of cure reactions of thermosetting systems. In this work, we applied thermal analysis to investigate the cure reaction of diglycidyl ether of bisphenol A-based epoxy resin as a function of the single-walled carbon nanotube (SWNT) concentration. The thermal characterization was performed using differential scanning calorimetry (DSC) and thermogravimetry (TGA). The vibrational properties of the composites at several nanotube concentrations were studied by Raman spectroscopy.

Correspondence to: J. M. Kenny.

Journal of Applied Polymer Science, Vol. 88, 452–458 (2003)

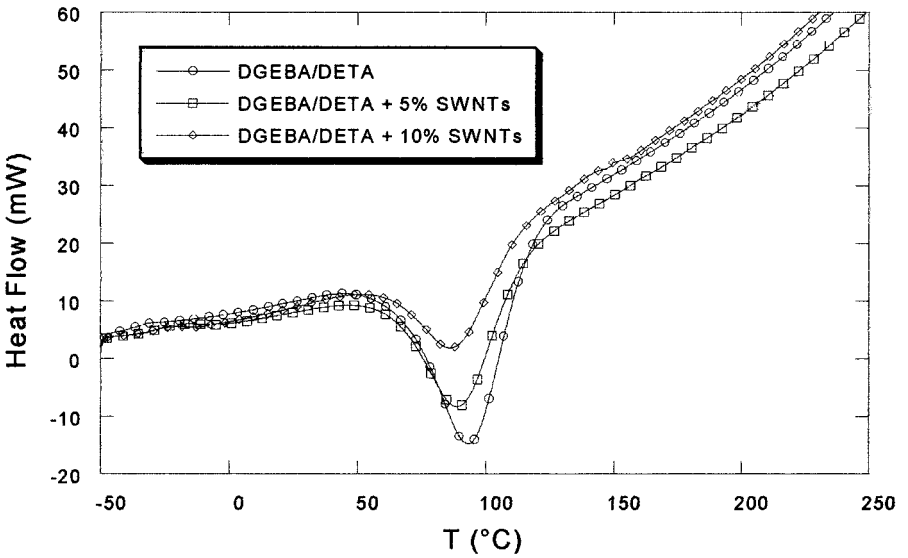

Figure 1 Dynamic DSC curves at a heating rate of 10°C/min for DGEBA/DETA and DGEBA/DETA–SWNT composites.

EXPERIMENTAL

A commercially available grade of a diglycidyl ether of bisphenol A-based (DGEBA) epoxy resin (epoxy equivalent weight 187) and a diethylenetriamine (DETA) hardener supplied by Sigma–Aldrich Chemicals (Italy) were used in this research. CarboLex AP-grade nanotubes (SWNTs) were provided by CarboLex (Lexington, KY). The material consists of packed bundles of SWNTs 12–20 Å in diameter. There are about 30 nanotubes per bundle (with an average bundle diameter of 100 Å) with a length of several micrometers.

For the composite production, SWNTs were sonically dispersed for 2 h in the liquid epoxy resin before curing. All samples were then cured with DETA with a stoichiometric weight ratio of DETA/DGEBA = 1: 7248, using a cure schedule with a temperature ramp from 30 to 150°C at a heating rate of 10°C/min. Two concentrations of nanotubes were analyzed: 5 and 10% specified as the weight phr with respect to the cured resin.

Isothermal and nonisothermal tests were performed using a DSC Perkin–Elmer Pyris 1 coupled with an intercooler. The standard procedure performed in nonisothermal scans was the following: Samples of about 10 mg were heated from −50 to 250°C at a scan rate of 10°C/min. Isothermal tests were performed at different temperatures (40, 50, 60, and 70°C) with a variable time depending on the stabilization of the cure reaction. Nonisothermal scans were then performed on the same samples to obtain the dynamic heat of reaction necessary to complete the cure of the reactive system.

Thermodegradation tests of DGEBA/DETA and DGEBA/DETA–SWNT composites were performed on approximately 10-mg samples in a Seiko Exstar 6000 TGA quartz rod microbalance. The tests were done in a nitrogen flow (200 mL/min) from 25 to 600°C with a 10°C/min heating ramp.

Raman scattering spectra were recorded by a Jobin Yvon micro-Raman LabRam system in a backscattering geometry. A 632.8-nm (1.96 eV) He–Ne laser with the power adjusted by optical filters was used as the light source. By using a 100× objective lens, the illuminated spot on the sample surface was focused to about a 2-μm diameter. The resolution of the Raman spectra was better than 1 cm^{-1}. SEM studies were performed on a Hitachi S800-FE operated at 30 kV.

RESULTS

The effects of SWNTs on the cure of the epoxy resin, analyzed by nonisothermal DSC experiments, are shown in Figure 1, where dynamic thermograms obtained on the neat DGEBA/DETA system and SWNT composites are reported. The total area under the thermogram, based on the extrapolated baseline at the end of the reaction, was used to calculate the total heat of reaction. The maximum of the exotherm peak (T_p) and the heat of reaction (ΔH_p) as a function of the SWNT concentration are reported in Table I. The relative shift of the T_p is well evident at the lowest reinforcement

TABLE I
Total Heat of Reaction and Maximum Reaction Peak Temperature of DGEBA/DETA System and DGEBA/DETA–SWNT Composites

System/composites	T_p (°C)	ΔH_p (J/g)
DGEBA/DETA	93.8	499
DGEBA/DETA + 5% SWNTs	89.8	465
DGEBA/DETA + 10% SWNTs	87.2	426

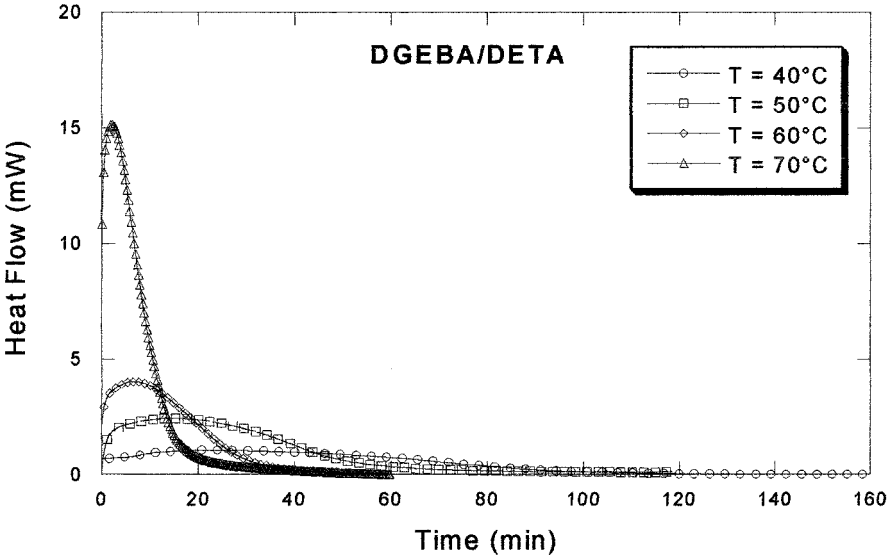

Figure 2 Isothermal DSC curves for DGEBA/DETA at different temperatures.

content with a slight but continuous further increase of the SWNT concentration. The decrease of the ΔH_p with increasing nanotube concentration can be directly attributed to the proportional reduction of the epoxy concentration in the composite.

The reaction rate $d\alpha/dt$ is directly proportional to the rate of heat generation dH/dt:

$$\frac{d\alpha}{dt} = \frac{1}{\Delta H_p}\frac{dH}{dt} \tag{1}$$

The extent of reaction α is given by:

$$\alpha = \frac{\Delta H_t}{\Delta H_p} \tag{2}$$

where ΔH_{pt} is the partial area under the DSC trace up to time t.

Heat flow versus time (t) at different isothermal temperatures for the DGEBA/DETA system and the 5% DGEBA/DETA–SWNT composite are shown in Figures 2 and 3. Similar results to those reported in Figure 3 were also obtained for the higher nanotube concentration (10% DGEBA/DETA–SWNT composite). The form of the curves reported in Figures 2 and 3 is typical of the isothermal reaction of thermosetting polymers. In fact, these systems are characterized by a maximum of the reaction rate at time zero, that is, when the concentration of reactive species is also maximum.[16] The shift of the maximum reaction rate observed in Figures 2 and 3 has been often associated to

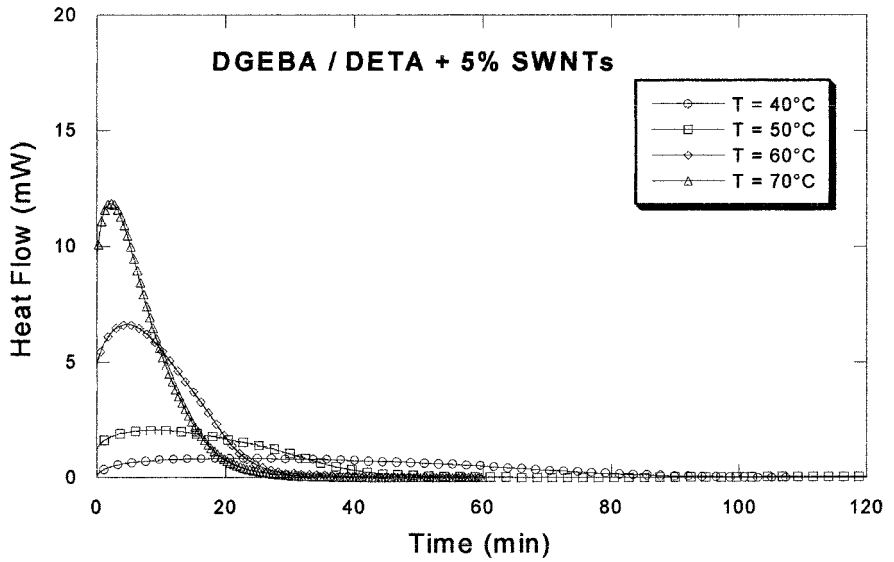

Figure 3 Isothermal DSC curves for 5% DGEBA/DETA–SWNT composite at different temperatures.

TABLE II
Time of the Maximum Reaction Rate for Isothermal Cure Tests at Different Temperatures of DGEBA/DETA System and DGEBA/DETA–SWNT Composites

T isothermal (°C)	T_{peak} (min) DGEBA/DETA	T_{peak} (min) DGEBA/DETA + 5% SWNTs	T_{peak} (min) DGEBA/DETA + 10% SWNTs
40	28.5	23.0	20.7
50	15.4	9.4	7.0
60	6.6	4.8	3.6
70	2.9	2.2	1.4

the "autocatalytic" behavior of DGEBA epoxy systems and their composites.[16] The time at the maximum reaction rate for different isothermal temperatures for the neat resin and their composites are reported in Table II, while the extent of reaction α versus time (t) at different isothermal temperatures is reported in Figure 4. From these values, it is evident that the acceleration effect of SWNT introduction on the rate of the reaction is more noticeable at low temperatures. Moreover, the well-known effects of the isothermal cure temperature on the final degree of the reaction of epoxy systems are detected in the Figure 4 results. However, no relevant effects of the presence of SWNTs on the maximum degree of cure of the epoxy are detected in the analyzed isothermal temperature range.

Thermogravimetric curves obtained for DGEBA and DGEBA–SWNT composites are reproduced in Figure 5, from which it can be seen that the DGEBA–SWNT composites exhibit a lower thermal stability. The higher weight loss is well evident at the lowest reinforcement content with a slight further decrease with the SWNT concentration.

Raman characterization was also applied to highlight the effects of SWNTs on the epoxy matrix composites. The high-frequency parts of the Raman spectra of the composites with the two SWNT concentrations studied (5 and 10%) are reported in Figure 6. The Raman bands of SWNTs are clearly observed in the DGEBA/DETA–SWNTs spectra but the DGEBA ones do not appear because of their low intensity. The spectra exhibit peaks at 1275, 1549, and 1589 cm^{-1}. The SWNT G modes (1549 and 1590 cm^{-1}) shown in Figure 6 involve tangential C—C bond stretching motions.[17] Generically, they stem from the E_{2g2} mode at 1580 cm^{-1} in graphite: $E_{2g_2} \rightarrow A_{1(g)} + E_{1(g)} + E_{2(g)}$. The graphitelike G modes exhibit a definite upward shift after the nanotubes were embedded in the epoxy matrix. The band localized around 1275 cm^{-1} is generally assigned to the D-line of the graphite and corresponds to the disordered graphite structures.[17–19] The D band is activated in the first-order scattering process of sp^2 carbons by the presence of in-plane substitutional heteroatoms, vacancies, a grain boundary, or other defects and by finite-size effects, all of which lower the crystalline symmetry of the quasi-infinite lattice.[17–19]

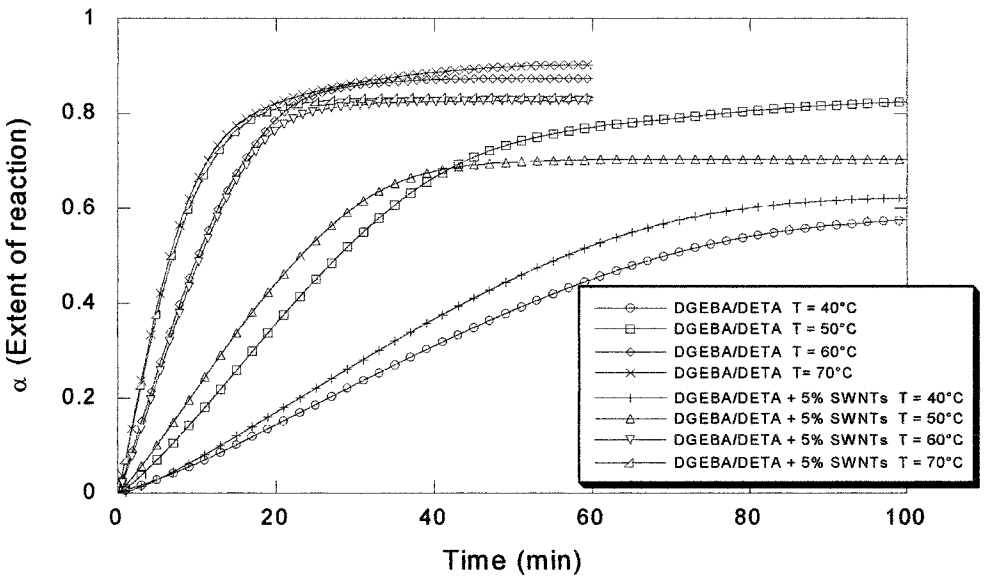

Figure 4 Extent of reaction α versus time at different isothermal temperatures for DGEBA/DETA system and 5% DGEBA/DETA–SWNT composite.

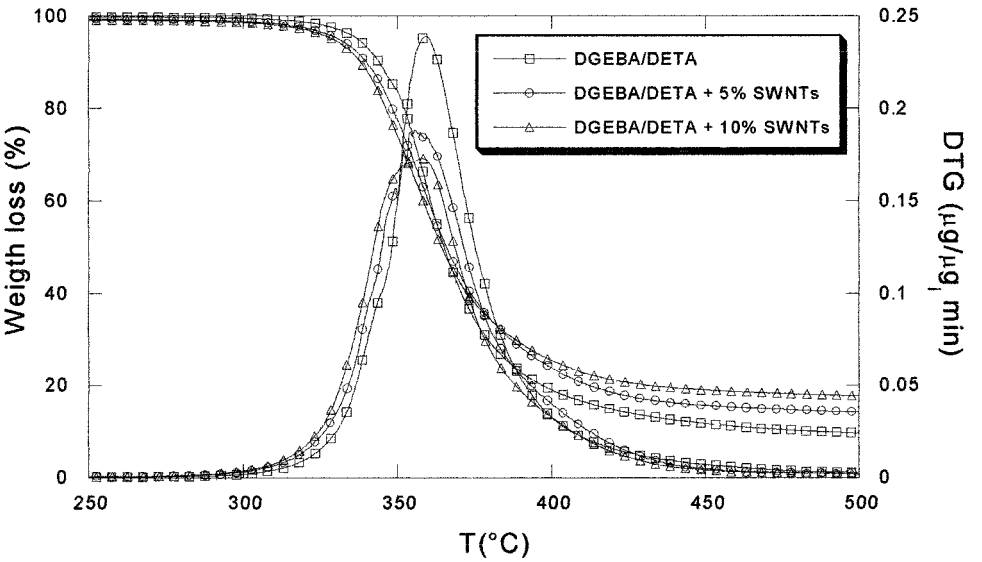

Figure 5 TG curves in nitrogen on heating ramp of 10°C/min of DGEBA/DETA system and DGEBA/DETA–SWNT composites.

The Raman spectra recorded on the same samples in the low-frequency part (Fig. 7) show a well-pronounced peak around 100–200 cm^{-1}. This band is attributed to the breathing-type vibration (RB modes, A_{1g} symmetry) of nanotubes and its frequency depends on the inverse diameter.[20–26] These spectra were then analyzed quantitatively by searching the minimum number of frequencies that fitted the different Raman bands without fixing the position and the widths of the individual peaks. By using this fitting procedure, three main features appear in the DGEBA/DETA–SWNT spectra at 145, 160, and 200 cm^{-1}. From Figure 8, it is clear that the mentioned peaks are upshifted when a low concentration of nanotubes is introduced into the DGEBA/DETA system, becoming then stable for 10% concentrations.

DISCUSSION

The observed microstructural changes induced by the incorporation of SWNTs are certainly a result of the modification occurring in the cure reaction. From the aforementioned findings, it is possible to relate the changes in cure kinetics, thermal degradation, and Raman spectroscopy of the SWNT composites to the dispersibility and particular thermal properties of the nanotubes. In fact, the extreme high thermal conductivity of carbon nanotubes can partially explain the observed accelerating effects on the curing kinetics and thermal degradation of the DGEBA/DETA–SWNT composites. However, the particular dependency of these processes on the concentration of the thermally active fillers can be explained only in terms

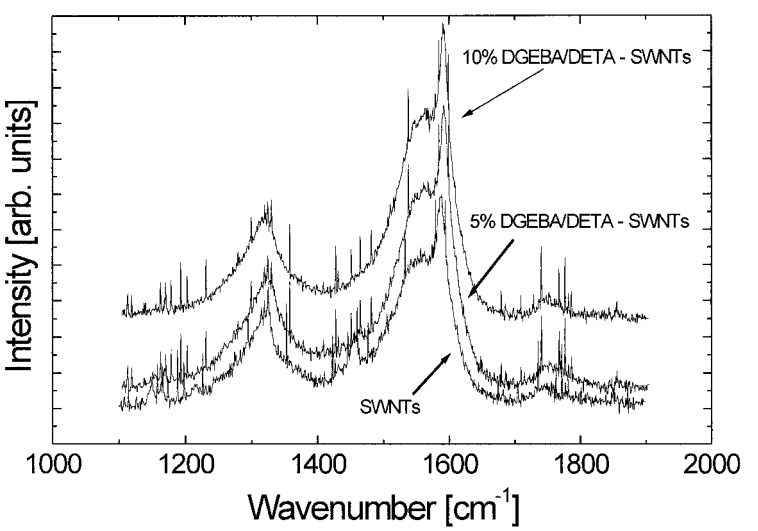

Figure 6 High-frequency Raman spectra of SWNTs and DGEBA/DETA–SWNT composites.

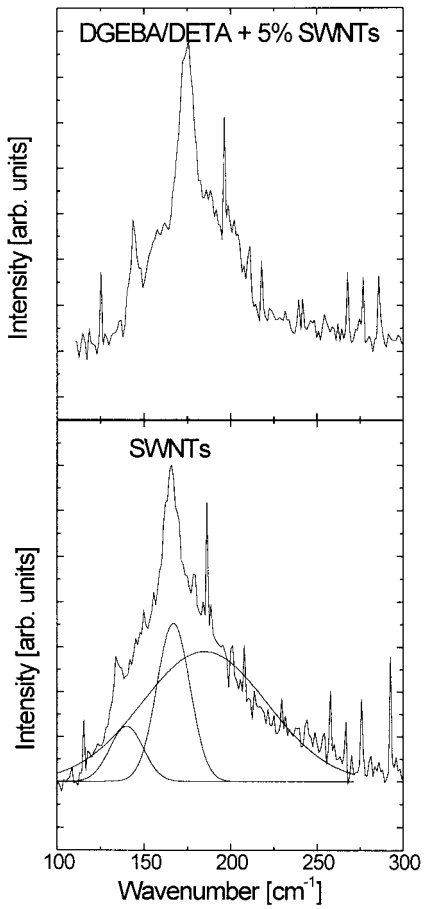

Figure 7 Low-frequency Raman spectra of SWNTs and DGEBA/DETA–SWNT composites.

of the ability of the epoxy resin to open and disperse the nanobundles. This conclusion is clearly supported by the Raman results, which suggests a direct association of the observed shift of the *G* modes with a coupling of SWNT bundles with the epoxy matrix. In particular, each peak from the decomposition of the low-frequency bands can be attributed to one nanotube diameter. Then, the shift of the Raman spectra peaks, especially the lower-frequency peaks, toward higher frequencies, when nanotubes are incorporated into the epoxy resin, can be explained by the opening of the nanotube bundles produced by the intercalation of the resin (Fig. 9). In fact, the resin now exerts a pressure on the dispersed individual tubes, increasing the breathing-mode frequencies.

The shift of the breathing modes can be related also to the modifications observed in the high-frequency bands.[26] In particular, it is possible to estimate the strain of the nanotubes and nanobundles due to epoxy shrinkage. We adopted the relative phonon frequency shift in the presence of the strain derived in ref. 27: $\Delta\omega^{\pm}/\omega_0 = -\gamma(1 - \nu_\tau)\varepsilon_z$, where γ is the Gruneisen parameter. The relative shift $\Delta\omega^{\pm}/\omega_0$ depends on the phonon eigenvector direction, and the splitting ($\Delta\omega^{+} - \Delta\omega^{-}$) is maximal for a chiral SWNTs, where $\Delta\omega^{+} = \Delta\omega^{A_{1g},E_{2g}}$ and $\Delta\omega^{-} = \Delta\omega^{E_{1g}}$. In chiral SWNTs, as those we likely tested in the Raman experiment, phonon displacements may have arbitrary directions with respect to the nanotube axis. Therefore, we observed an average shift of $\Delta\omega$ (1594 cm^{-1})/$\omega_0 = -\gamma(1 - \nu_\tau)\varepsilon_z$. The *G* band shifts ~3 cm^{-1} from SWNTs to the 5% SWNT composite. From the above-mentioned expression with $\Delta\omega$ (1594 cm^{-1}) = 3 cm^{-1}, γ = 1.24 (ref. 27), and ν_t = 0.28 (ref. 28), one readily finds $\varepsilon_z = -0.21\%$, which translates to a compressive strain of the nanoropes. A similar compressive strain was found for the 10% DGEBA/DETA–SWNT composite, suggesting that no further intercalation of the polymer and no further dispersion of the nanobundles occur at higher nanotube concentrations.

CONCLUSIONS

It has been demonstrated how the incorporation of SWNTs affects the cure reaction of the DGEBA epoxy matrix and this change is very important to interpret the function of the nanotubes as reinforcement in composite materials. It was observed that the rate of reaction and the thermal degradation increases with increasing SWNT concentration, these being effects already appreciable at the lower nanotube concentration analyzed (5%). A further increase of the SWNT concentration does not produce a proportional effect, suggesting a saturation of the nanotube incorporation.

The changes in cure kinetics, thermal degradation, and Raman spectroscopy of the SWNT composites can be interpreted in terms of the extreme high thermal conductivity of carbon nanotubes and the ability of the epoxy resin to open and disperse the nanobundles, offering a higher surface for heat propagation.

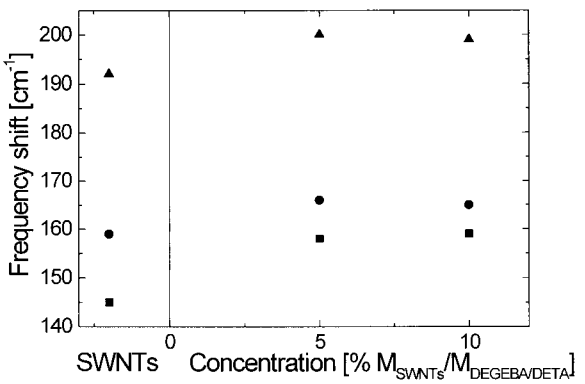

Figure 8 Decomposition of the low-frequency bands of DGEBA/DETA–SWNT composites for several concentrations.

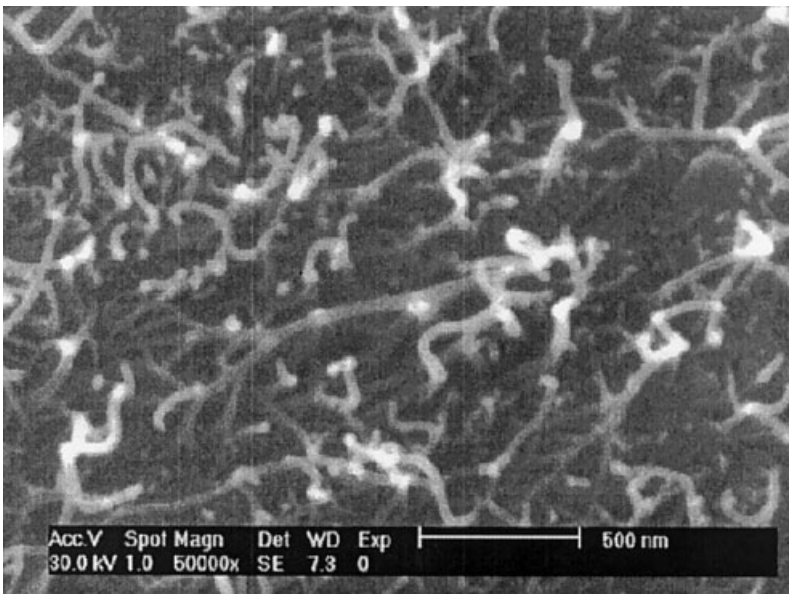

Figure 9 SEM image of 5% DGEBA/DETA–SWNT composite.

References

1. Ijjima, S. Nature 1991, 354, 56.
2. Rinzler, A. G.; Hafner, J. H.; Nikolaev, P.; Lou, L.; Kim, S. G.; Tomanek, D.; Nordander, P.; Cobert, D. T.; Smalley, R. E. Science 1995, 269, 1550.
3. De Heer, W. A.; Chatelain, A.; Ugarte, D. Science 1995, 270, 1179.
4. Collins, P. G.; Zettl, A.; Bando, H.; Thess, A.; Smalley, R. E. Science 1997, 278, 100.
5. Wagner, H. D.; Lourie, O.; Feldman, Y.; Tenne, R. Appl Phys Lett 1998, 72, 188.
6. Dagani, R. Chem Eng News 1999, 7, 25.
7. Wang, Z. L.; Poncharal, P.; de Heer, W. A. In First IUPAC Workshop on Advanced Materials: Nanostructured Systems, Hong Kong, July 14–18, 1999.
8. Curran, S; Ajayan, P.; Blau, W.; Carrol, D.; Coleman, J.; Dalton, A.; Davey, A. P.; McCarthy, B.; Stevens, A. Adv Mater 1998, 10, 1091.
9. Alexandre, M.; Dubois, P. Mater Sci Eng 2000, 28, 1.
10. Thostenson, E. T.; Ren, Z.; Chou, T. W. Compos Sci Technol 2001, 61, 1899.
11. Sandler, J.; Shaffer, M. S. P.; Prasse, T.; Bauhofer, W.; Schutle, K.; Windle, A. H. Polymer 1999, 40, 5967.
12. Schadler, L. S.; Giannaris, S. C.; Ajayan, P. M. Appl Phys Lett 1998, 73, 3842.
13. Cooper, C. A.; Young, R. J.; Halsall, M. Composite Part A 2000, 32, 401.
14. Rosenberg, B. A. Adv Polym Sci 1986, 75, 113.
15. Peyser, P.; Bascom, W. D. J Appl Polym Sci 1977.
16. Kenny, J. M. J Appl Polym Sci 1994, 51, 761–1433.
17. Saito, R.; Dresselhaus, G.; Dresselhaus, M. S. Physical Properties of Carbon Nanotubes; Imperial College: London, 1998.
18. Rao, A. M.; Jorio, A.; Pimenta, M. A.; Dantas, M. S.; Saito, R.; Dresselhaus, G.; Dresselhaus, M. S. Phys Rev Lett 2000, 84, 1820.
19. Brown, S. D.; Jorio, A.; Dresselhaus, G.; Dresselhaus, M. S. Phys Rev B 2000, 64, 73403.
20. Bandow, S. Phys Rev Lett 1998, 80, 3779.
21. McNamara, K. M. J Appl Phys 1994, 76, 2466.
22. De la Chappelle, M. L.; Lefrant, S.; Journet, C.; Maser, W.; Bernier, P.; Loiseau, A. Carbon 1998, 36, 705.
23. Eklund, P. C.; Holden, J. M.; Jishi, R. A. Carbon 1995, 33, 959.
24. Rao, A. M.; Richter, E.; Bandow, S.; Chase, B.; Eklund, P. C.; Williams, K. A.; Fang, S.; Subbaswamy, K. R.; Menon, M.; Thess, A.; Smalley, R. E.; Dresselhaus, G.; Dresselhaus, M. S. Science 1997, 275, 187.
25. Rinzler, A. G.; Liu, J.; Dai, H.; Nikolaev, P.; Huffman, C. B.; Rodriguez-Macias, F. J.; Boul, P. J.; Lu, A. H.; Heymann, D.; Colbert, D. T.; Lee, R. S.; Fischer, J. E.; Rao, A. M.; Eklund, P. C.; Smalley, R. E. Appl Phys A 1998, 67, 29.
26. Iliev, M. N.; Litvinchuk, A. P.; Arepalli, S.; Nikolaev, P.; Scott, C. D. Chem Phys Lett 2000, 316, 217.
27. Reich, S.; Jantoliak, H.; Thomsen, C. Phys Rev B 2000, 61, 13389.
28. Lu, J. P. Phys Rev Lett 1997, 79, 1297.